Original Paper

Indoor+Built Environment

Indoor Built Environ 2000;9:182–191

Accepted: May 31, 2000

A Macroscopic Model for Predicting Dust Concentration Distribution in Swine Buildings

M.C. Puma[a] R.G. Maghirang[b]

[a]Department of Agricultural and Biosystems Engineering, Iowa State University, Ames, Iowa,
[b]Department of Biological and Agricultural Engineering, Kansas State University, Manhattan, Kans., USA

Key Words
Air quality · Dust · Modelling · Agricultural buildings

Abstract
A macroscopic model for predicting dust concentration distribution in mechanically ventilated swine rooms has been developed. The model accounts for the effect of turbulent diffusive deposition, gravitational settling, coagulation and ventilation. Four particle diameter size ranges were chosen to represent the fine particles in swine buildings: 0.5–0.9, 0.9–1.6, 1.6–2.8, and 2.8–5.0 µm. Predicted results indicated that ventilation would be the dominant particle removal mechanism accounting for over 90% of the particles removed; that deposition of particles on surfaces would be small (2–9%), and loss by coagulation negligible (≈0%). Additionally, source location would strongly influence the dust concentration distribution in the prototype swine room. Dust generation rate and presence or absence of obstructions in the form of mock pigs would affect the dust distribution minimally. Temperature difference between supply and room air (7–9 vs. 14–16°C) would not cause any appreciable difference in dust distribution.

Introduction

There has been limited research to investigate dust transport within livestock buildings. Such research is needed to gain a better understanding of the transport and removal of particulate contaminants within these facilities. A recent trend in the analysis of air contaminant transport in ventilated spaces is toward numerical modelling, which involves either microscopic or macroscopic models. Microscopic models are used to examine the details of air and contaminant movement within an airspace. Macroscopic models, on the other hand, are employed to estimate particle concentration for a microenvironment.

A lumped-parameter model for describing the dynamics of airborne dust at any location within a ventilated space was developed and evaluated by Liao and Feddes [1–3]. It was based on the population-balance model, which is a basic way to describe the time-dependent change in properties of airborne dust undergoing turbulent coagulation, turbulent diffusive deposition and gravitational settling and while being moved by ventilation airflow [1]. In the model the removal of dust was represented by three dimensionless parameters that characterized the relative effects of turbulent coagulation, turbulent diffu-

KARGER
Fax + 41 61 306 12 34
E-Mail karger@karger.ch
www.karger.com

1420–326X/00/0094–0182$17.50/0

Accessible online at:
www.karger.com/journals/ibe

Dr. M.C. Puma
130 Davidson Hall
Ames, IA 50011 (USA)
Tel. +1 515 292 7967, Fax +1 515 294 9973, E-Mail mpuma@iastate.edu

sive deposition and gravitational deposition. Three model cases, i.e., complete mixing, displacement system and short circuiting, were studied. Results from the model indicated that the displacement ventilation system was more effective than the short circuiting system in removing dust. Predicted dust concentrations compared well with experimental data. Nazaroff and Cass [4, 5] also developed a general mathematical model for predicting the concentrations and fate of particulate matter in indoor air that considered the effects of ventilation, air cleaning, deposition, direct emission and coagulation, based on the population-balance model. The model determined not only the total concentrations of aerosol material components but also concentrations of defined particle sizes. The authors simulated the patterns of particle size distribution in a small ventilated chamber and found good agreement between predicted and experimental results. They also assessed the soiling rates of paintings in museums due to deposition of small particles and used the model to assess air quality in office rooms and residential buildings. Offermann et al. [6] used a macroscopic model to describe particle removal performance of air cleaners as a function of particle diameter and the mean room concentration.

The present study details the implementation of a simplified macroscopic model for predicting dust concentrations, size distribution patterns and particle transport in a simulated swine room. The relative contributions of gravitational settling, coagulation and ventilation on the removal of particulate contaminants from the swine room have been determined. The effect of ventilation rate, dust generation rate, temperature difference between supply and room air, source location, and the presence or absence of obstructions, in the form of mock pigs, on dust concentration distribution were also evaluated.

Methods

Model Development

A macroscopic model has been developed for predicting dust concentrations and particle size distribution in mechanically ventilated swine rooms based on the general mathematical model formulated by Nazaroff and Cass [4, 5] and the lumped-parameter modelling approach of Liao and Feddes [1–3]. The model will account for the effects of ventilation, deposition onto surfaces, coagulation and direct emission of particles.

The swine room was represented as a set of 16 interconnected chambers or control volumes each having a well-mixed core (fig. 1). Applying the model, for each control volume, p and particle size range, q, the rate of change in dust mass concentration can be written as:

$$\frac{dC_{pq}}{dt} = S_{pq} - (LC)_{pq} \tag{1}$$

where C_{pq} = mass concentration of dust particles within size range q in control volume p ($\mu g \cdot m^{-3}$); S_{pq} = production or emission rate of dust particles within size range q in control volume p ($\mu g \cdot m^{-3}\ s^{-1}$); L_{pq} = loss or removal rate of particles within size range q in control volume p (s^{-1}); q = 1,2...,n where n is the total number of particle size ranges, and p = 1,2...,m where m is the total number of control volumes.

The parameter S_{pq} is considered to include direct emission inside the ventilated space (E), advective transport from the ventilation system or from outside air (A), and coagulation of particles (K). The room was assumed windowless, airtight and with well-insulated wall and ceiling surfaces so that advection from outside air could be neglected. The parameter L_{pq} is considered to include removal by ventilation (R), particle losses to surfaces by deposition (D), and loss to a larger size by coagulation (K′). Dust removal by airflow movement due to ventilation was represented by:

$$\frac{dC_{pq}}{dt} = \sum_{x=1} \frac{(f_{xp}C_{xq} - f_{px}C_{pq})}{V_p} \tag{2}$$

where f_{xp} = volumetric airflow rate from adjacent control volumes or from ventilation system to control volume p ($m^3 \cdot s^{-1}$); C_{xq} = mass concentration of particles in size range q in the adjacent control volumes or in the ventilation system supply air ($\mu g \cdot m^{-3}$); f_{px} = volumetric airflow rate from control volume p to the adjacent control volumes or to the exhaust outlet ($m^3 \cdot s^{-1}$); C_{pq} = mass concentration of particles in size range q in control volume p ($\mu g \cdot m^{-3}$), and V_p = volume of control volume p (m^3).

The volumetric airflow rates, f_{px} and f_{xp}, were determined from preliminary experiments in which air velocities between the control volumes, from the ventilation air supply diffuser to the adjoining control volume, and from an adjoining control volume to the outlet were measured. Then, taking small cross-sectional areas between boundaries of the coplanar boundaries between control volumes, cross-flow ventilation rates between control volumes were estimated by multiplying the measured air velocities with the cross-sectional areas of the coplanar boundaries. Details of the experimental procedures and results have been thoroughly discussed elsewhere [7–9].

The rate of change of dust concentration due to deposition was estimated from the equation:

$$\frac{dC_{pq}}{dt} = -\left(\frac{C_{pq}}{V_p}\right) \sum_{m=1} (V_{dmq}A_m) \tag{3}$$

where V_{dmq} = mean deposition velocity of particles within size range q during deposition to the m^{th} surface of control volume p ($m \cdot s^{-1}$) and A_m = superficial area of the m^{th} surface of control volume p (m^2).

The mean deposition velocity, V_{dmq}, was estimated for three possible airflow regimes in the chamber: (1) natural convection driven by temperature differences between the surfaces (floor, walls, ceiling) and the nearby air; (2) homogeneous turbulence in the core of the room, and (3) forced laminar flow parallel to the surface. Equations relating deposition velocity to particle size, surface characteristics (orientation, temperature, velocity of nearby air), and flow condi-

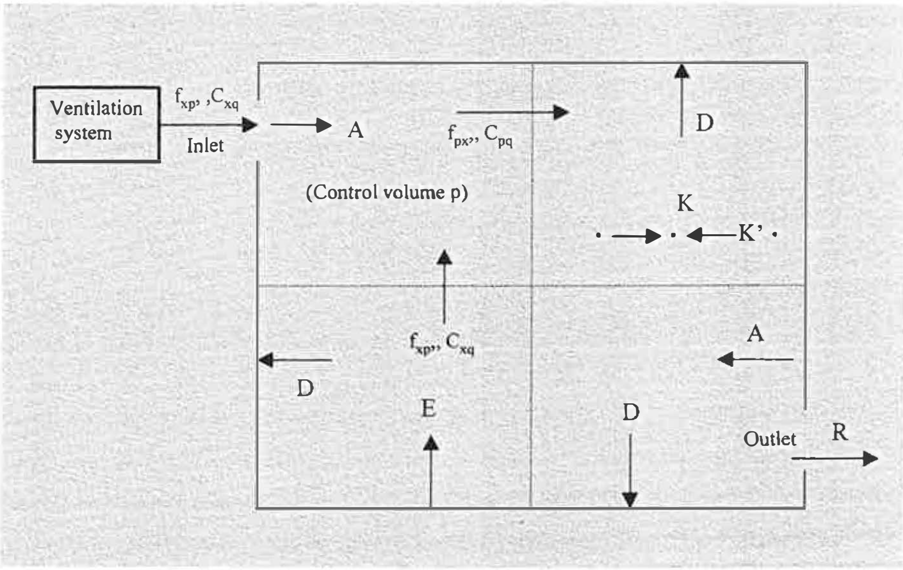

Fig. 1. Schematic diagram of the components of the dust concentration model. C_{pq} = Concentration of dust particles within size range q in control volume p; C_{xq} = concentration of dust particles within size range q in adjacent control volumes; E = direct emission from sources in ventilated airspace; A = advective transport from the ventilation system or from outside air; K = coagulation from smaller particles; K' = loss to a larger size due to coagulation; D = deposition losses to surfaces (floor, walls, ceiling); R = removal by ventilation; f_{xp} = volumetric airflow rate from adjacent control volumes or from ventilation system to control volume p; f_{px} = volumetric airflow rate from control volume p to adjacent control volumes or to exhaust outlet; q = 1,2,...r (r is total number of sections/particle size range); p = 1,2,...s (s is the total number of control volumes).

tions were obtained from published values [4, 5, 10, 11]. For example, the deposition velocity for a particle with diameter d_p being deposited on a horizontal upward facing surface (e.g., floor) due to homogeneous turbulence can be estimated by:

$$V_d = V_{cp} + V_t \tag{4}$$

where

$$V_t = N_t \nu \frac{\left(\dfrac{K_e}{\alpha}\right)^{1/2}}{\tan^{-1}\left[\delta\left(\dfrac{K_e}{\alpha}\right)^{1/2}\right]} \tag{5}$$

and

$$V_{cp} = \frac{V_g}{\left[1 - \exp\left(-\dfrac{\Pi}{2}\dfrac{V_g}{(DK_e)^{1/2}}\right)\right]} \tag{6}$$

where V_{cp} = deposition velocity due to combined effects of eddy diffusion, Brownian motion, advection and gravitational settling ($m \cdot s^{-1}$); V_t = deposition velocity due to effect of thermophoresis ($m \cdot s^{-1}$); N_t = thermophoresis parameter (dimensionless), = $K(\Delta T/T_a)$; ΔT = temperature of surface, T_s, minus temperature of air outside boundary layer, T_α, (K); K = thermophoresis coefficient (dimensionless); ν = kinematic viscosity of air, ($m^2 \cdot s^{-1}$); K_e = turbulence intensity parameter (s^{-1}); α = thermal diffusivity of air ($m^2 \cdot s^{-1}$); δ = boundary layer thickness (m), = $(1.2)(\nu/K_e)^{4/9} X_s^{1/9}$; X_s = length of the surface in the direction of flow (m); V_g = gravitational settling velocity ($m \cdot s^{-1}$), and D = coefficient of Brownian diffusivity of particles ($m^2 \cdot s^{-1}$).

The thermophoresis coefficient, K, depends on particle size and, for particles larger than the mean free path of air molecules, on the ratio of thermal conductivity of the gas to that of the particle (K_g/K_p). A formula for estimating K has been given by Nazaroff and Cass [4]. For particles in air with $d_p \leq 3.0$ µm and K_g/K_p in the range of 0.01–0.50, K varies between 0.10 and 0.60. A representative value of K is 0.50, particularly for particles smaller than 1 µm [4]. The turbulence intensity parameter, K_e, has the dimension of inverse time and is obtained from a fit to experimental data on the measured deposition flux to the surface of the enclosure. Effect of coagulation was treated in the model using the following equation [5]:

$$\frac{dC_{pq}}{dt} = \frac{1}{2}\left[\sum_{r=1}^{q-1}\left(\sum_{s=1}^{q-1}[[{}^{1}\overline{\beta}_{rsq}]C_{ps}C_{pr} - \left(\sum_{r=1}^{q-1}[[{}^{2a}\overline{\beta}_{rq}]C_{pq}C_{pr}\right) - \right.\right.$$
$$\left.\left.[{}^{2b}\overline{\beta}_{rq}]C_{pr}C_{pq}]\right) - \frac{1}{2}[{}^{3}\overline{\beta}_{qq}](C_{pq})^2 - C_{pq}\left[\sum_{r=q+1}^{u}[{}^{4}\overline{\beta}_{rq}]C_{pr}\right] \tag{7}$$

where $\overline{\beta}_{rsq}$ = mean rate of collision between dust particles in sections r and s yielding particles in the size range/section q, and sections r and s were sections/size ranges smaller than q ($m^3 \cdot \mu g^{-1} \cdot s^{-1}$); $\overline{\beta}_{rq}$ = mean rate of collision between dust particles in sections r and q yielding particles in section q or a section larger than q ($m^3 \cdot \mu g^{-1} \cdot s^{-1}$); $\overline{\beta}_{qq}$ = mean rate of collision between dust particles in section q yielding particles larger than q ($m^3 \cdot \mu g^{-1} \cdot s^{-1}$); C_{ps}, C_{pr}, C_{pq} = mass concentrations of dust particles contained within control volume p in size range/section s, r, q, respectively ($\mu g \cdot m^{-3}$), and u = total number of particle size ranges/sections.

The superscripts 1, 2a, 2b, 3, and 4 in equation 7 represent the possible types of collision between particles. For a given size range q, four classes of collisions are possible, with the type of collision distinguished by the sizes of the colliding particles: (1) two particles, each from a size range smaller than q (e.g., size ranges r and s), collide to produce a particle in size range q (valid for $1 < q \leq n$); (2) one particle from a size range smaller than q collides with a particle in size range q to yield either a particle in size range larger than q or a particle in size range q (valid for $1 < q \leq n$); (3) two particles in size range q collide to yield a particle in a size range larger than q (valid for $1 \leq q < n$), and (4) a particle in q collides with a particle in a size range larger than q (valid for $1 \leq q < n$).

Equations 2, 3, and 7 were combined with the direct emission term and cast into the form of equation 1. The equations were solved numerically using the asymptotic integration method [12]. For each

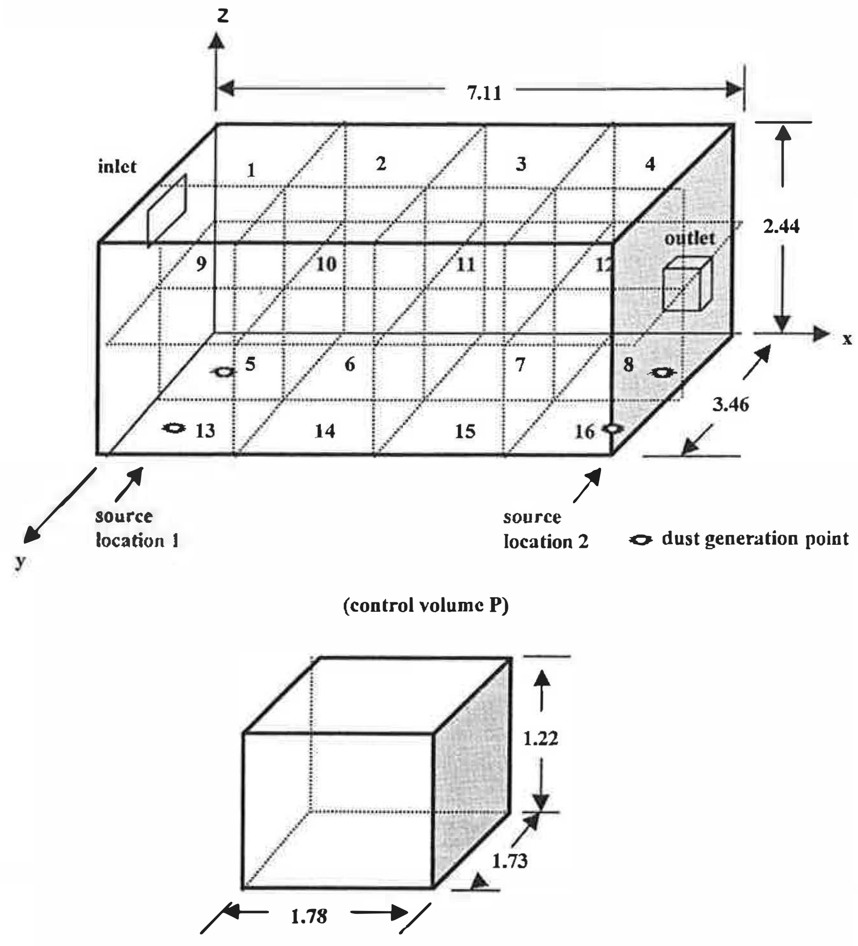

Fig. 2. Schematic diagram of the prototype swine room used in the numerical modeling (all units in m, not drawn to scale).

section, the initial indoor dust mass concentration and the hourly averaged values of outdoor dust mass concentration were specified. Direct indoor emissions at constant rates were also specified as hourly-averaged values.

The program, written in FORTRAN-77, was contained in 10 files comprising 70 subroutines and functions. It was executed by first preparing an input file that contained a list of commands including input data using a text editor and then compiling and linking the 10 program files. Most of the simulations required 1–2 min of CPU time on a SUNSPARC station 10 or 20 with a SUN operating system version 5.5.1.

Assumptions and Limitations of the Model

Model simulation assumed the following: (1) the swine room can be represented by 16 control volumes, each with a well-mixed core; (2) particles are spherical and have equal densities, and (3) the particle mass concentration is uniformly distributed with respect to the logarithm of the mass or diameter of the particle.

Implementation of the Model

The model was implemented on a prototype room (7.11 m wide, 3.46 m long and 2.44 m high) representing typical mechanically ventilated swine nursery rooms (fig. 2). The room had a rectangular air supply diffuser on one sidewall and an exhaust opening on the opposite wall. The room was divided into 16 zones or control volumes with each control volume measuring 1.78 × 1.73 × 1.22 m. Four particle size ranges were chosen to represent the fine particles: 0.5–0.9, 0.9–1.6, 1.6–2.8, and 2.8–5.0 μm.

Sixteen test cases involving combinations of two levels of ventilation rates, three airflow thermal conditions, two dust generation rates, two source locations, and the presence or absence of obstructions were studied (table 1). The airflow thermal conditions were isothermal, nonisothermal (no heat load), and nonisothermal (with heat load). A heat load of 1,600 W representing the metabolic heat generation of the pigs was provided for the non-isothermal (with heat load) test cases.

Isothermal test cases (test cases 1–4, 11 and 12) had a ventilation rate of 0.336 $m^3 \cdot s^{-1}$; temperatures of supply and room air, which

Table 1. Description of the 16 test cases

Test case No.	Ventilation rate $m^3 \cdot s^{-1}$	Airflow thermal condition[1]	Dust generation rate[2]	Obstruction	Source location[3]
1	0.336	isothermal	low	without	1
2	0.336	isothermal	low	with	1
3	0.336	isothermal	high	without	1
4	0.336	isothermal	high	with	1
5	0.096	nonisothermal, no heat load	low	without	1
6	0.096	nonisothermal, no heat load	low	with	1
7	0.096	nonisothermal, no heat load	high	without	1
8	0.096	nonisothermal, no heat load	high	with	1
9	0.096	nonisothermal, with heat load	low	with	1
10	0.096	nonisothermal, with heat load	high	with	1
11	0.336	isothermal	high	without	2
12	0.336	isothermal	high	with	2
13	0.096	nonisothermal, no heat load	high	without	2
14	0.096	nonisothermal, no heat load	high	with	2
15	0.096	nonisothermal, with heat load	low	with	2
16	0.096	nonisothermal, with heat load	high	with	2

[1] For the isothermal condition, supply (T_o) and room air (T_i) temperatures varied from 24 to 27°C. For the nonisothermal, no heat load condition, temperature difference between supply and room air was 7–9°C. For the nonisothermal, with heat load condition, temperature difference was 14–16°C.
[2] Low dust generation rate = 201–248 $\mu g \cdot min^{-1}$; high dust generation rate = 270–335 $\mu g \cdot min^{-1}$.
[3] 1 = Source location near the inlet; 2 = source location near the exhaust.

were almost the same for each case, varied from 24 to 27°C. Nonisothermal (no heat load) test cases (test cases 5–8, 13 and 14) had a ventilation rate of 0.096 $m^3 \cdot s^{-1}$; air temperature differences between supply and room air ranged from 7 to 9°C. Nonisothermal (with heat load) test cases (test cases 9, 10, 15 and 16) had a ventilation rate of 0.096 $m^3 \cdot s^{-1}$; air temperature differences varied from 14 to 16°C. The two ventilation rates: 0.336 $m^3 \cdot s^{-1}$ for isothermal test cases and 0.096 $m^3 \cdot s^{-1}$ for the non-isothermal test cases, were close to the recommended ventilation rates of 0.341 and 0.067 $m^3 \cdot s^{-1}$ for nursery pigs weighing 13.6–34.1 kg during mild and cold weather, respectively [13].

Dust generation rates were high (270–335 $\mu g \cdot min^{-1}$) or low (201–248 $\mu g \cdot min^{-1}$). Two source locations were considered: source location 1 was near the supply diffuser; source location 2 was near the exhaust (fig. 2). Obstructions were represented by 'mock pigs', in the form of 16 galvanized steel tubes (2.80 m long and 20.3 cm in diameter), which were uniformly distributed in the test room. These mock pigs were present for test cases that had obstructions and removed for test cases without obstructions.

Data Analysis

The predicted dust mass concentrations were normalized using the procedure suggested by Kato and Murakami [14] to account for differences in dust generation rates:

$$C_p^*(t) = \frac{C_{pq}(t) - C_{iq}(t)}{\left[\frac{G_q(t)}{Q}\right] - C_{oq}(t)} \tag{8}$$

where $C_{pq}^*(t)$ = normalized concentration of dust particles within size range q in control volume p at time t (dimensionless); $C_{pq}(t)$ = predicted concentration of dust particles within size range q in control volume p at time t ($\mu g \cdot m^{-3}$); $C_{iq}(t)$ = concentration of dust particles within size range q at the inlet at time t ($\mu g \cdot m^{-3}$); $G_q(t)$ = generation rate of particles within size range q at time t ($\mu g \cdot s^{-1}$); $C_{oq}(t)$ = concentration of dust particles within size range q at the exhaust at time t ($\mu g \cdot m^{-3}$), and Q = ventilation rate ($m^3 \cdot s^{-1}$).

Model Validation

To verify the predicted results, controlled laboratory tests using a full-scale room air distribution chamber were conducted. Details of the experimental procedure and results have been presented elsewhere [7–9]. A summary of the procedures is presented below.

Experiments were conducted in a full-scale test chamber similar to the prototype room (fig. 2) for validating the predicted results. The chamber had a cross-flow jet ventilation system with air entering a rectangular air supply diffuser on one sidewall and exhausted by a variable speed fan mounted on the opposite sidewall. A furnace filter was installed at the air supply diffuser to filter out particles coming in from the ventilation system. For the nonisothermal test cases, outside air was first conditioned through a 7.44-$kW \cdot h^{-1}$ air conditioner.

Cornstarch powder served as the test dust material because corn constitutes the bulk of most swine rations. The material has a wider range of particle sizes than swine house dust but exhibits some of the characteristics (chemical makeup and density) of swine house dust. Particle density of the test dust was determined to be 1.6 $g \cdot cm^{-3}$. To disperse the material a dust generator originally developed at the Bureau of Standards was used. The dust generator was placed outside the chamber because it might have modified the airflow pattern if it had been sited within the chamber. The dust particles were emitted into the airstream through two plastic tubes, one on each side of the chamber, with the end of each tube set at 0.2 m above the floor (fig. 2).

A microprocessor-controlled optical particle counter monitored the dust concentrations. It was placed outside the chamber and connected to a manifold system to enable automatic measurements from 16 locations. Attached to the manifold was a multiple sampling port placed at the center of the room that enabled continuous measurements from the 16 locations without interference with the airflow inside the room. Dust concentration was measured at the center of each control volume. Sampling time was 15 s for each control volume and sampling between any two control volumes was 15 s. It took 8 min to measure the concentrations at all 16 control volumes during each reading. Readings were at 15-min interval starting from the beginning of dust generation for 1.5 or 2 h during which time steady-state concentrations in the control volumes were attained.

The inside surfaces of the chamber were cleaned thoroughly before each test. The surfaces were wiped with wet mops and the ventilation system was run for several hours to remove airborne dust. A test was started only when the dust concentrations in the control volumes were about the same as the outdoor concentrations. Initial dust concentrations inside the chamber were measured before the start of each dust generation. After dust generation was started, dust concentrations were read at 15-min interval until steady-state concentrations were attained (i.e., when concentrations were at levels ± 5% of previous reading). Measured dust concentrations were normalized using the same procedure used for normalizing predicted concentrations.

Results

Results from representative test cases are presented below to show the performance of the model. For all test cases, predicted concentrations were symmetric about the x-z plane or the longitudinal (x) axis of the chambers so that only half of the chamber was considered. Additionally, predicted values for the 0.5- to 0.9-, 0.9- to 1.6-, 1.6- to 2.8-μm particle size ranges and total dust (0.5–5.0 μm) agreed well with measured values [8, 9]. Measured values for the 2.8- to 5.0-μm particle sizes were higher than predicted values; it was suspected that this was due to an error in measurement of the concentrations of the 2.8- to 5.0-μm particle range.

Table 2. Dust particle removal (percentage of total)[1]

Test case No.	Ventilation	Deposition
1	95	5
2	98	2
3	94	6
4	98	2
5	91	9
6	91	9
7	92	8
8	92	8
9	92	8
10	94	6
11	97	3
12	96	4
13	94	6
14	93	7
15	92	8
16	93	7

[1] Loss due to coagulation was negligible (≈0%) for all test cases.

Dust Removal Mechanisms

Predicted values indicated that, for all test cases, dust removal by ventilation was the dominant mechanism (19–98%); removal by deposition of particles on surfaces was 2–9%; removal by coagulation (≈0%) was negligible (table 2).

Effects of Ventilation Rate, Temperature Difference, Dust Source Location and Obstructions

Isothermal Case

Normalized predicted concentrations for the eight control volumes (control volumes 1–8) for test case 1 are shown in figure 3. Test case 1 involved an isothermal test condition, low dust generation rate, dust generation at source location 1 (near control volume 5), and without the mock pigs in the chamber. Concentrations immediately increased from the initial values to levels approximating the steady-state values after the first 15 min of the simulation (fig. 3). During this period, normalized values increased from 0 to 0.80 for control volumes 1–4 and 6–8, and from 0 to 1.10 for control volume 5. For all control volumes, differences in the predicted concentrations for the four particle size ranges (0.5–0.9, 0.9–1.6, 1.6–2.8,

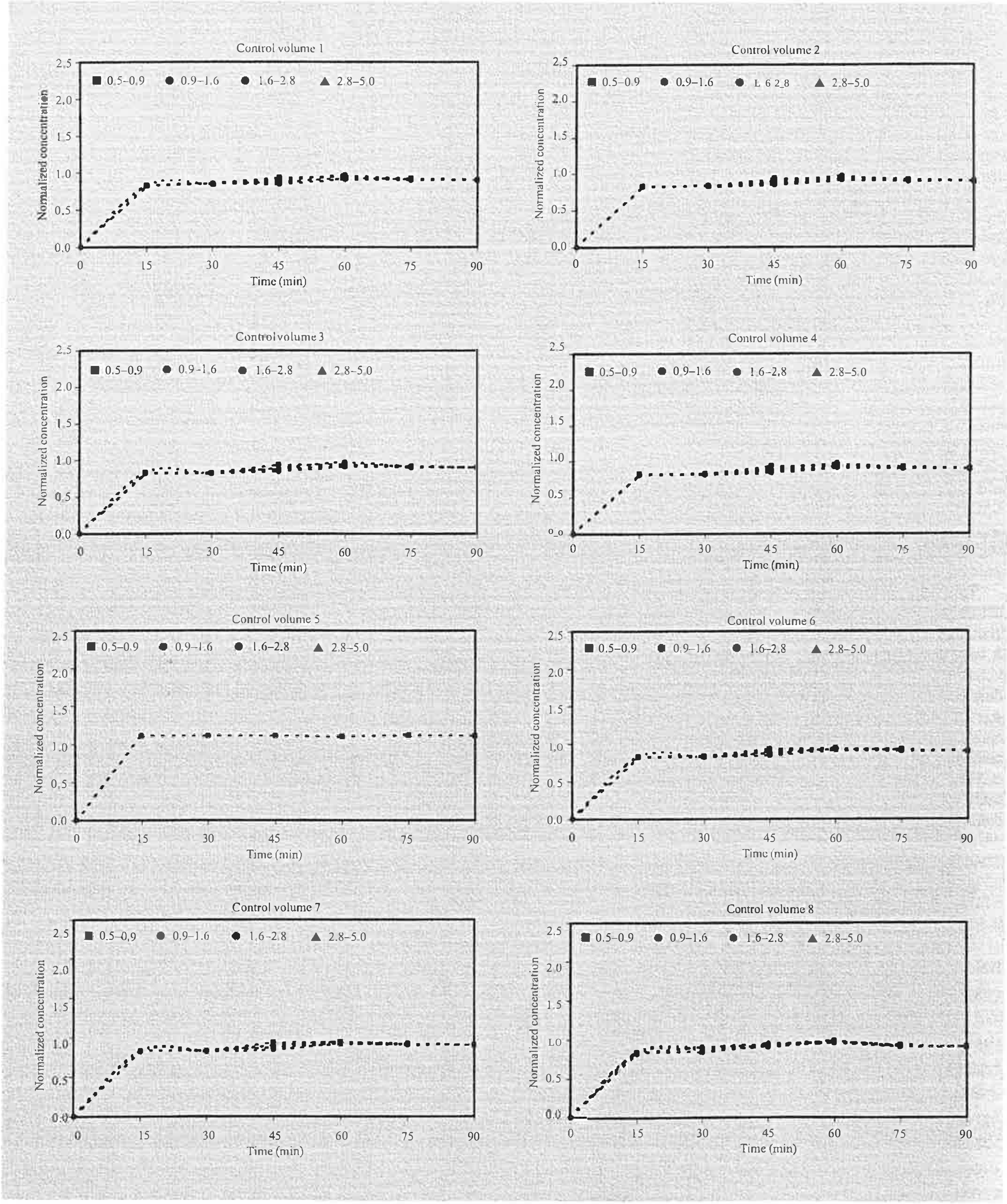

Fig. 3. Variations of normalized predicted dust concentrations (by particle size range) with time (test case 1).

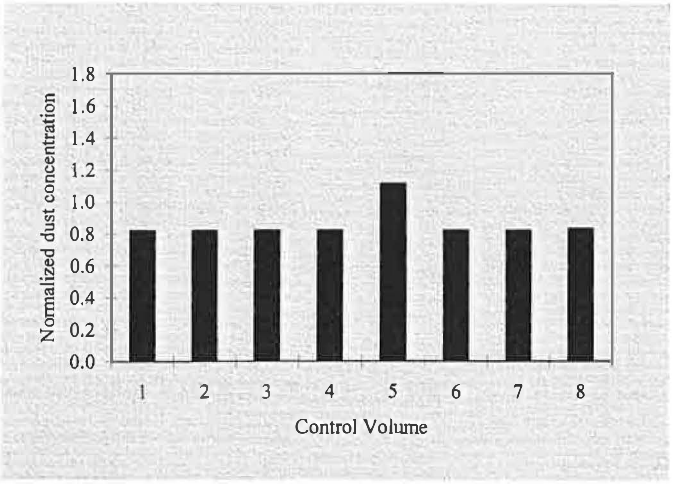

Fig. 4. Predicted total dust concentrations for test case 1 (isothermal, low dust generation rate, without mock pigs, source location 1).

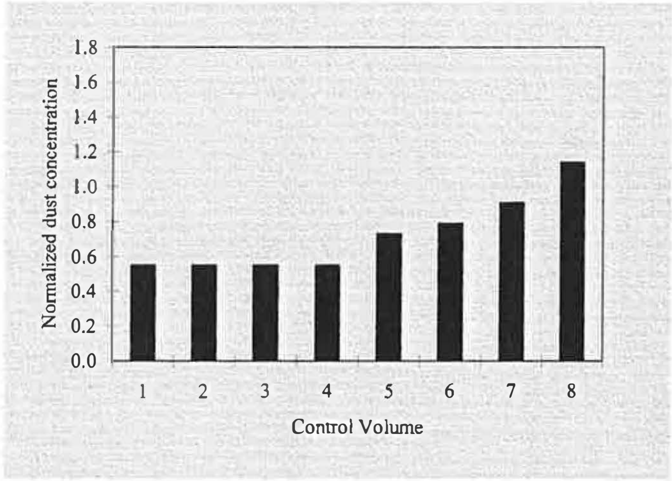

Fig. 5. Predicted total dust concentrations for test case 11 (isothermal, high dust generation rate, without mock pigs, source location 2).

and 2.8–5.0 μm) were minimal. Normalized values then increased gradually until the steady-state levels were reached in about 90 min. Steady-state normalized concentrations ranged from 0.82 to 0.83 for control volumes 1–4 and 6–8, and 1.11 for control volume 5 (fig. 4). Predicted concentrations were higher for control volume 5 than for all the other control volumes.

Similar trends were observed on the predicted concentrations of test cases 2–4. All these test cases had dust generation also at source location 1. Test case 2 differed from test case 1 only in having mock pigs inside the chamber. Test cases 3 and 4 were similar to test cases 1 and 2, respectively, but involved higher dust generation rates. The similarity in the trends of predicted dust concentrations between test case 1 and those of test cases 2–4 indicated that dust generation rate and presence of the mock pigs did not have much influence on the dust concentration distribution in the room. The mock pigs occupied only a small portion (≈2.3%) of the control volumes so that the airflow and dust transport between the control volumes were not affected by their presence. Regarding the effect of the dust generation rate, the actual values of dust concentrations were higher for test cases with higher dust generation rates; however, normalized values were almost the same.

Predicted values for test cases involving source location 2 (test cases 11 and 12) also showed small differences in the predicted values for the four particle size ranges. However, the trend for dust concentrations among control volumes was different from test cases involving source location 1. The steady-state normalized predicted total dust concentrations for test case 11 (isothermal, low dust generation rate, without mock pigs, source location 2) is shown in figure 5. Normalized concentrations for the upper control volumes (control volumes 1–4) were lower than values for the lower control volumes (control volumes 5–7). Predicted concentration was higher for control volume 8 (the dust source location) than for all the other control volumes. Differences in the predicted concentrations between test cases involving source location 1 with those involving source location 2, as shown in figures 4 and 5, indicated that source location exerted a strong influence on dust particle concentration distribution.

Nonisothermal (No Heat Load) Test Cases

Model predictions under this condition are presented by the results for test case 5 [nonisothermal (no heat load) condition, low dust generation, without the mock pigs, and dust source location 1]. For this test case, there were small variations in the predicted values for the eight control volumes. Likewise, there were small differences in the predicted concentrations for the four particle size ranges. The steady-state normalized predicted total dust concentrations for control volumes 2–4 and 6–8 ranged from 0.98 to 0.99 (fig. 6). For control volume 5, the source location control volume, steady-state normalized concentration was 1.00. For control volume 1, which was above control volume 5 but directly in front of the air supply

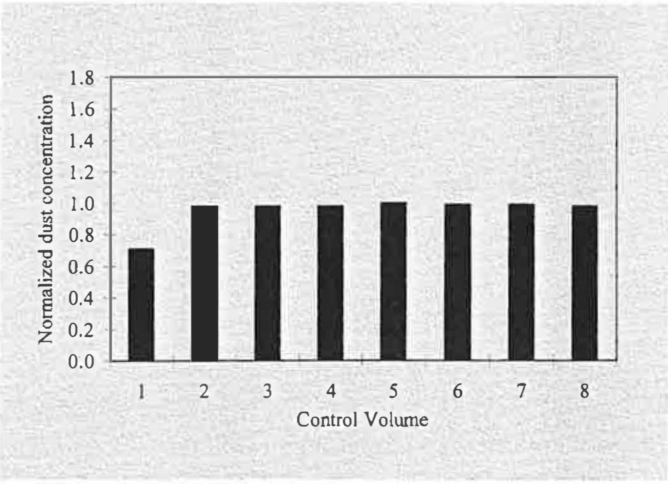

Fig. 6. Predicted total dust concentrations for test case 5 (nonisothermal, low dust generation rate, without mock pigs, source location 1).

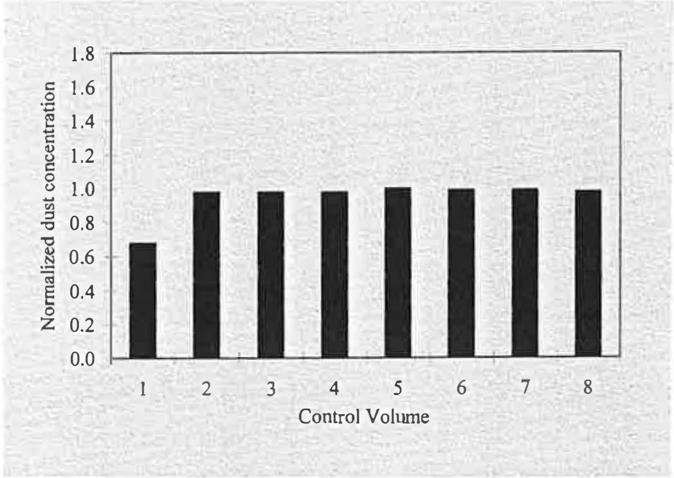

Fig. 7. Predicted total dust concentrations for test case 9 (nonisothermal, low dust generation rate, with mock pigs, source location 1).

diffuser, steady-state value was 0.71. Almost the same variations were obtained for the other test cases involving the same thermal condition and source location, but either with higher dust generation and with the presence of mock pigs in the room (test cases 6–8). Again, this indicated a minimal effect of dust generation rate and the presence or absence of mock pigs on the dust concentration distribution.

For test cases that had source location 2 (test cases 13 and 14), normalized concentrations showed an increasing trend for the upper control volumes (from control volume 1–4). For the lower control volumes, normalized concentrations increased from control volume 5–8. This difference in predicted dust concentration distribution with those of test cases 5–8 was due to the effects of difference in source location.

Nonisothermal (with Heat Load) Test Cases

For these test cases, there were also small variations in the predicted concentrations among the eight control volumes and between the four particle size ranges. The steady-state normalized total dust concentrations for test case 9 [nonisothermal (with heat load), low dust generation rate, with mock pigs, and dust source location 1] are shown in figure 7. Values for control volumes 2–4 and 6–8 were almost the same (0.98). For control volume 5 (source location), normalized value was just slightly higher (1.00), while for control volume 1, it was 0.68. The trends of the predicted values for test case 10 followed those of test case 9. This trend was similar to that of the nonisothermal (no heat load) test cases (fig. 5), indicating that temperature difference between supply and room air was not enough to cause any appreciable difference in room dust distribution.

Results of test cases 15 and 16, which involved source location 2, indicated increasing concentrations for both the upper and lower control volumes. This trend was also similar to that of the corresponding nonisothermal (no heat load) test cases.

Summary and Conclusions

A general macroscopic model that accounted for convective diffusion, coagulation, and gravitational sedimentation was implemented to determine the dust concentration distribution in a typical mechanically ventilated swine nursery room as affected by ventilation rate, temperature difference between supply and room air, dust generation rate, and the presence or absence of mock pigs. The following conclusions were drawn:

(1) Ventilation was the dominant dust particle removal mechanism, accounting for 91–98% of the total dust removed. Deposition of particles on wall, ceiling and floor surfaces (2–9 %) was small, and the effect of coagulation (≈0%) was negligible.

(2) Source location had a strong influence on dust concentration distribution. Dust concentrations tended to be higher at the source location control volumes than in all other control volumes.

(3) Obstructions (i.e., mock pigs) and dust generation rates had little influence on dust distribution.

(4) The temperature difference between supply and room air (7–9 vs. 14–16 °C) was not enough to cause any appreciable difference in dust distribution.

Acknowledgments

The contribution of Dr. William W. Nazaroff, Mr. Steve Coulson, and Dr. Murali Narayanan is acknowledged. Support from the Kansas Agricultural Experiment Station (AES Contribution No. 00-236-J) is also acknowledged.

References

1 Liao CM, Feddes JJR: Mathematical analysis of a lumped-parameter model for describing the behaviour of airborne dust in animal housing. Appl Math Modelling, 1990;14:248–257.
2 Liao CM, Feddes JJR: Modelling and analysis of airborne dust removal from a ventilated airspace. Can Agric Eng 1991;33:355–361.
3 Liao CM, Feddes JJR: A lumped parameter model for predicting airborne dust concentrations in a ventilated airspace. Trans Am Soc Agric Engineers 1992;35:1973–1978.
4 Nazaroff WW, Cass GR: Mathematical modelling of chemically reactive pollutants in indoor air. Environ Sci Technol 1986;20:924–934.
5 Nazaroff WW, Cass GR: Mathematical modelling of indoor aerosol dynamics. Environ Sci and Technol 1989;23:157–166.
6 Offermann FJ, Sextro RG, Fisk WJ, Grimsrud, DT, Nazaroff WW, Nero A, Rexzan KL, Yater J: Control of respirable particles in indoor air with portable air cleaners. Atmos Environ 1985;19:1761–1771.
7 Puma MC: Modelling Dust Concentration Distribution in Swine Houses; PhD diss Kansas State University, Manhattan, Kansas, 1998.
8 Puma MC, Maghirang RG, Hosni MH, Hagen L: Modelling dust concentration distribution in a swine house under isothermal conditions. Trans Am Soc Agric Engineers 1999;42:1811–1821.
9 Puma MC, Maghirang RG, Hosni MH, Hagen L: Modelling dust concentration distribution in a swine house under non-isothermal conditions. Trans Am Soc Agric Engineers 1999;42: 1823–1832.
10 Incropera FP, DeWitt DP: Fundamentals of Heat and Mass Transfer. J. New York, Wiley, 1985.
11 Corner J, Pendlebury ED: The coagulation ad deposition of stirred aerosol. Proc Phys Soc 1951;B64:645–654.
12 Young TR, Boris JP: A numerical technique for solving stiff ordinary differential equations associated with the chemical kinetics of reactive-flow problems. J Phys Chem 1977;81: 2424–2427.
13 Midwest Plan Service: Mechanical ventilating systems for livestock housing. MWPS-32. Ames, Midwest Plan Service, 1990.
14 Kato S, Murakami S: New ventilation efficiency scales based on spatial distribution of contaminant concentration aided by numerical simulation. Trans Am Soc Heating Refrigeration Air Conditioning Engineers 1995;94:309–330.